EPJ Web of Conferences **172**, 01001 (2018) https://doi.org/10.1051/epjconf/201817201001
*ISMD 2017*

# PHENIX Measurements of Heavy Flavor in Small Systems

*Alexandre* Lebedev[1,⋆]

[1] *Iowa State University, Ames, IA 50011-3160, USA*

**Abstract.** The study of heavy flavor production in proton-nucleus and nucleus-nucleus collisions is a sensitive probe of the hot and dense matter created in such collisions. Installation of silicon vertex detectors in the PHENIX experiment, and increased performance of the BNL RHIC collider allowed collection of large amount of data on heavy flavor production in small colliding systems.
In this talk we will present recent PHENIX results on open heavy flavor and quarkonia production in p+p, p+A, d+A, and He3+A colliding systems in a broad rapidity range, and discuss how these measurements help us to better understand all stages of nuclear collisions at high energy.

## 1 $J/\psi$ polarization in $p+p$ collisions at $\sqrt{s} = 510$ GeV

In most genaral case the angular distribution of the positive lepton from the $J/\psi$ decay can be written as

$$\frac{dN}{d\cos\theta d\phi} \propto 1 + \lambda_\theta \cos^2\theta + \lambda_{\theta\phi} \sin 2\theta \cos\phi + \lambda_\phi \sin^2\theta \cos 2\phi \quad (1)$$

where $\lambda_\theta$ is the polar, $\lambda_\phi$ is the azimuthal, and $\lambda_{\theta\phi}$ is the "mixed" angular decay coefficients.

The angles $\phi$ and $\theta$ are measured relative to a reference frame defined such that the $\hat{x}$ and $\hat{z}$-axes lie in the production plane, formed by the momenta of the colliding protons and the particle produced. The direction of the $\hat{z}$-axis within the production plane is arbitrary. The simplest frame to study the particle wave function is the one in which the density matrix has only diagonal elements, or the single and double spin-flip terms are zero. This simplest frame is also called the natural frame and is identified when the azimuthal coefficients in (1) are zero. The three most common frames used in particle angular distribution studies are (Fig. 1):

The Helicity frame (HX) [1], traditionally used in collider experiments, takes the $\hat{z}$-axis as the spin-1 particle momentum direction

The Collins-Soper frame (CS) [2], widely used in Drell-Yan measurements, choses the $\hat{z}$-axis as the difference between the momenta of the colliding hadrons boosted into the spin-1 particle rest frame

⋆e-mail: lebedev@iastate.edu

The Gottfried-Jackson frame (GJ) [3], typically used in fixed target experiments, takes the $\hat{z}$-axis as the beam momentum boosted into the spin-1 particle rest frame. At forward angles in a collider environment, the definition of the GJ frame depends heavily on which beam is used in the definition. If the beam circulating in the same direction as the $J/\psi$ momentum is chosen (GJ forward), the resulting $\hat{z}$-axis is nearly collinear with the $\hat{z}$-axis of the HX and CS frames and points in the same direction. In GJ backward frame (beam circulating in the direction opposite to $J/\psi$ momentum is chosen) the $\hat{z}$-axis points in the opposite direction.

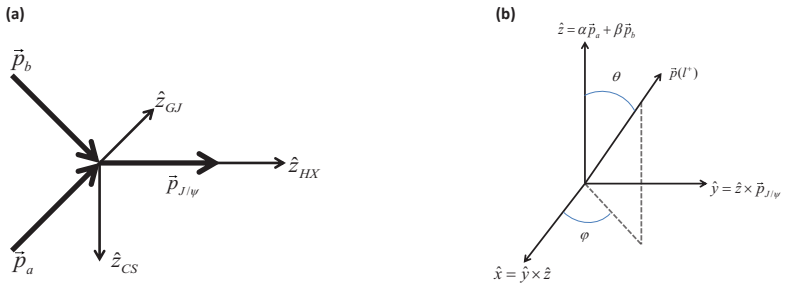


**Figure 1.** Reference frames and coordinate system used in this analysis. The $\hat{x}$ and $\hat{z}$-axes are chosen to lie in the production plane determined by the colliding hadrons and the particle produced (a $J/\psi$ in this figure) with momenta $\vec{p}_a$, $\vec{p}_b$ and $\vec{p}_{J/\psi}$. The left diagram shows the production plane and the direction convention for the $\hat{z}$ in the Collins-Soper (CS), Helicity (HX) and Gottfried-Jackson (GJ) reference frames. The angles $\theta$ and $\phi$ in the diagram on the right represent the direction of the positive decay lepton in the corresponding reference frame.

$J/\psi$ mesons were reconstructed by calculating the invariant mass of all unlike-sign muon pairs after analysis cuts. Combinatorial random background was estimated by like-sign dimuons calculated as $2\sqrt{N^{++}N^{--}}$, where $N^{++}$ and $N^{--}$ are number of positive and negative same-sign pairs respectively, and subtracted. Mass distributions for each bin in $p_T$ and rapidity are then fit using a double Gaussian as signal and exponential background in order to remove dimuons from Drell-Yan and correlated open-heavy flavor decays. The number of $J/\psi$'s is obtained directly by integrating the dimuon invariant mass distribution in a mass interval from 2.5 to 3.7 GeV/$c^2$ after background subtraction. Background subtraction was performed for each individual $\cos\theta$-$\phi$ bin.

The $J/\psi$ angular distributions are divided into 12 bins in $\cos\theta$ and 10 bins in $\phi$. Combinatorial and correlated background is subtracted bin-by-bin, and angular distributions are then corrected for acceptance, which is calculated assuming no polarization, that is $\lambda_\theta = \lambda_{\theta\phi} = \lambda_\phi = 0$. This is done for each of the three transverse momentum bins in each polarization frame. The angular decay coefficients obtained in this way were used in the next iteration to calculate acceptance, and the procedure was repeated until it converged.

The resulting angular decay coefficient $\lambda_\theta$ and frame-independent coefficient $\tilde{\lambda}$ are shown in Fig. 2 and Fig. 3 respectively, for four reference frames as a function of transverse momentum. In all frames the polar coefficient $\lambda_\theta$ is strongly negative at low $p_T$ and becomes close to zero at high $p_T$, while the azimuthal coefficient $\lambda_\phi$ is close to zero at low $p_T$, and becomes slightly negative at high $p_T$. The frame-independent coefficient $\tilde{\lambda}$ is strongly negative at all $p_T$ in all frames.

The measured polar coefficient $\lambda_\theta$ is compared to theoretical prediction for prompt $J/\psi$ in Helicity frame calculated in the NRQCD factorization by H. .S. Chung et al, [4] and H. Shao et al., [5] in

Fig. 2. At high $p_T$ both predicitions are in good agreement with the data, while at low $p_T$ a strong deviation can be seen. No theoretical calculation is available for the frame-independent coefficient $\tilde{\lambda}$ or for other reference frames. The reported experimental results represent a challenge for the theory and provide a basis for better understanding of quarkonium production in high energy $p+p$ collisions.

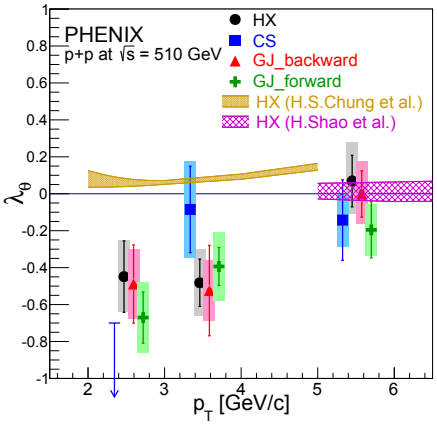


**Figure 2.** Polar angular decay coefficient $\lambda_\theta$ as a function of transverse mometum for four reference frames and three $p_T$ bins. Black circles: HX frame; blue squares: CS frame; red triangles: GJ Backward; green crosses: GJ Forward frames. Shaded error boxes show systematic uncertainty. Points are shifted in $p_T$ for clarity. Down-pointing arrow indicates 90% confidence limit. The data are compared with NRQCD theorectcal predictions in Helicity frame by H. S. Chung et al. [4] and H. Shao et al. [5].

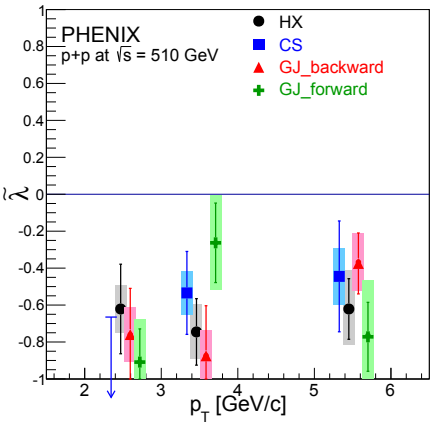


**Figure 3.** Frame-independent angular decay coefficient $\tilde{\lambda}$ as a function of transverse mometum for the four reference frames and three $p_T$ bins. Black circles: HX frame; blue squares: CS frame; red triangles: GJ Backward; green crosses: GJ Forward frames. Shaded error boxes show systematic uncertainty. Points are shifted in $p_T$ for clarity. Down pointing arrow indicates 90% confidence limit.

## 2 $J/\psi$ and $\psi(2S)$ in $p/d/He^3 + Al/Au$ collisions at $\sqrt{s} = 200$ GeV

Heavy charm quarks are produced in initial hard scatterings, and their production can be calulated in perturbative QCD approach, so the initial state effects are well under control. $c\bar{c}$ pairs form $J/\psi$ and $\psi(2S)$ at the later stages of the collisions. Binding energies of these two charmonium states are very different (640MeV and 50MeV). Thus, the difference between these two states can help us to understand the final state effiects in nucleus-nucleus collisions.

The PHENIX experiment has measured [7] previously $\psi(2S)$ nuclear modification factor in d+Au collisions at $\sqrt{s} = 200$ GeV/$c$. That measurement was done at mid-rapidity. The magnitude and the trend with centraility of $\psi(2S)$ meson suppression turned out to be very different than that of $J/\psi$ [6]. In most central d+Au collisions $\psi(2S)$ suppression was measured to be almost 3 times larger than that of $J/\psi$. Since the initial state factors in a nucleus, such as shadowing and energy loss, should be the same or very similar for $c\bar{c}$ precursor pairs for both $\psi(2S)$ and $J/\psi$, something different must be happening in the later stages of the collision. This measurement became possible after installation of the Forward Silicon Vertex Detector (FVTX), which allowed better mass resolution by precisely measuring opening angle of an opposite sign muon pair.

The new PHENIX measurement of $\psi(2S)$ production in p+p, p+Au and p+Al collisions at $\sqrt{s}$ = 200 GeV/$c$ at forward/bacward rapidity may shed light on the relatively large suppression of $\psi(2S)$. Fig. 4 shows the fraction of $\psi(2S)/J/\psi$ as a function of transverse momentum ($p_T$) in proton-proton collisions. Integrated over all $p_T$, this fraction is around 2%, which is in agreement with the world data at different $\sqrt{s}$. Fig. 5 compares the new PHENIX result at forward rapidity (solid black circles) with the PHENIX result at mid-rapidity (open gray circles) and world data as a function of transverse momentum. The green band in Fig. 5 shows Color Evaporation Model (CEM) prediction. The $p + p$ measurement serves as a baseline for calculating nuclear modification factor in the proton-nucleus collisions.

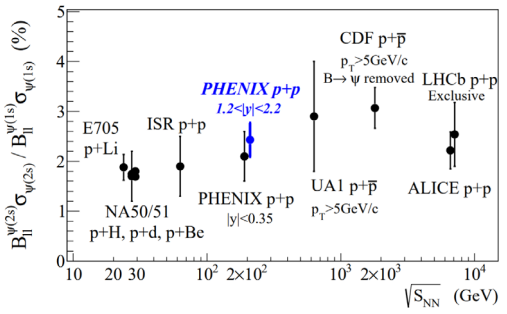


**Figure 4.** Comparison of world data on the ratio of $\psi(2S)/J/\psi$ mesons in di-lepton decays as a function of $\sqrt{s}$ in proton-proton collisions.

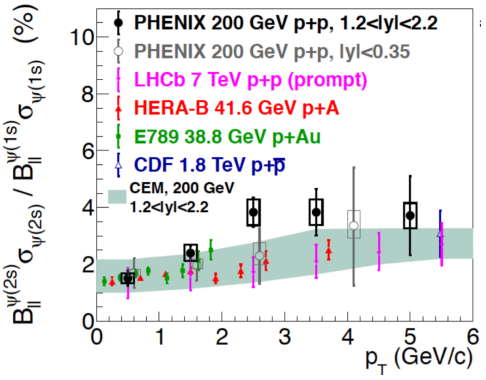


**Figure 5.** Comparison of world data on the ratio of $\psi(2S)/J/\psi$ mesons as a function of $p_T$ along with calculation from a color evaporation model (green band).

Fig. 6 shows relative suppression of $\psi(2S)/J/\psi$ as a function of rapidity for p+Au and p+Al collisions, as well as the old d+Au result at mid-rapidity. In the proton-going direction (positive rapidity) suppression of $\psi(2S)$ is, essentially, the same as that of $J/\psi$, while in the nucleus-going direction (negative rapidity) $\psi(2S)$ are much more suppressed both in p+Au and p+Al collisions. In other words, $\psi(2S)$'s are strongly suppressed in both directions, while $J/\psi$'s are strongly suppressed in proton-going direction, and moderately in nucleus-going direction. The same figure also shows a calculation based on breakup by co-moving particles (dashed lines). The calculation qualitatively explains the observed rapidity dependence, but underestimated the magnitude.

Fig. 7 shows relative suppression of $\psi(2S)/J/\psi$ as a function of co-mover density, which is expressed as particle multiplicity $dN/d\eta$ divided by nuclear overlap $< S_T >$, calculated using Glauber model. The results obtained by the ALICE experiment [8], and LHCb experiments also show the increased suppression with increasing co-mover density observed by the PHENIX experiment.

## 3 Open charm and bottom via di-electrons in $p + p$ and $d + Au$ collisions

Beauty production in p+p collisions at $\sqrt{s}$ = 200 GeV was studied using opposite sign di-electrons using simultaneous fit of invariant mass and transverse momentum distributions [9]. The spectrum of di-electrons produced in p+p collisions is well understood in terms of hadronic cocktail (at low mass) and Drell-Yan, charm, and beauty decays (at high mass). After the yield from vector, pseudo-scalar mesons, and Drell-Yan is subtracted from the measured di-electron spectrum, we are left with

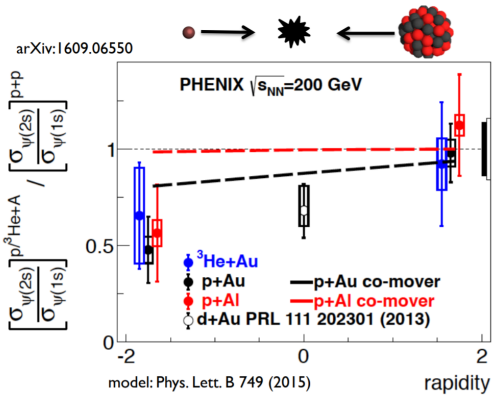


**Figure 6.** The double ratio of $\psi(2S)/J/\psi$ mesons measured in $p/d/^3He + A$ collisions to the same ratio in $p+p$ collisions as a function of rapidity, along with a calculation based on breakup by co-moving particles.

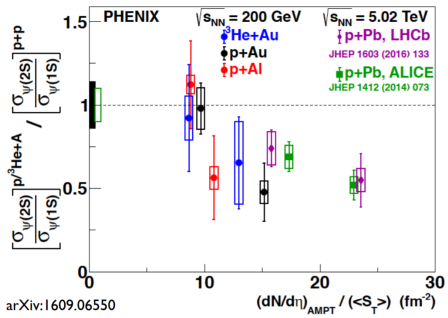


**Figure 7.** The double ratio of $\psi(2S)/J/\psi$ mesons measured in $p/^3He + A$ collisions to the same ratio in $p + p$ collisions as a function of co-moving particle density.

di-elctrons from semi-leptonic decays of charm and beauty. The main idea behind charm/beauty separation is that di-electrons from charm dominate low invariant mass and low $p_T$ region of this two-dimasional space, while di-electrons from beauty dominate either high mass and low $p_T$, or low mass and high $p_T$ regions. One-dimensional projections of two-dimensional fits to invariant mass axis are shown in Fig. 8.

This approach is model-dependent, since the decay electron spectra depend on original charm/beauty distributions. However, for heavier quarks (beauty) the effect of the original quark distribution gets smeared by the decay kinematics, and the results do not depend on the chosen model. This is not true in case of charm. We used three models, tuned PYTHIA [10], POWHEG [11], and MC@NLO [12] to check model deendence of the results.

The integrated $c\bar{c}$ and $b\bar{b}$ cross-sections obtained for $p + p$ and $d + Au$ collisions are shown in Fig. 9. The $b\bar{b}$ cross-section shows, as expected, no model dependence, while $c\bar{c}$ cross-section is strongly dependent on rapidity shape of the original quark distribution, which is different in PYTHIA, POWHEG, and MC@NLO. The same model dependence is seen for both $p + p$ and $d + Au$ collisions.

We also looked at the ratio (or nuclear modification factor) of cross-sections of $c\bar{c}$ and $b\bar{b}$ in $d + Au$ and $p + p$ collisions, and this is shown in Fig. 10. This ratio is similar for all the event generators and no deviation from unity is observed.

## 4 Conclusions

We have reviewed recent PHENIX measurements of heavy flavor in small systems.

First full measurement of $J/\psi$ polarization at RHIC energies represents a challenge to theory and could provide a basis for better understanding of quarkonia production mechanisms.

A wealth of data on $J/\psi$ and $\psi(2S)$ production show enhanced relative suppression of $\psi(2S)$ in nucleus-going direction. Qualitatively it can explained by co-mover dissociation.

Charm and bottom cross-section measurement in $p+p$ and $d+Au$ shows no significant modification in $d + Au$ within experimental uncertainties.

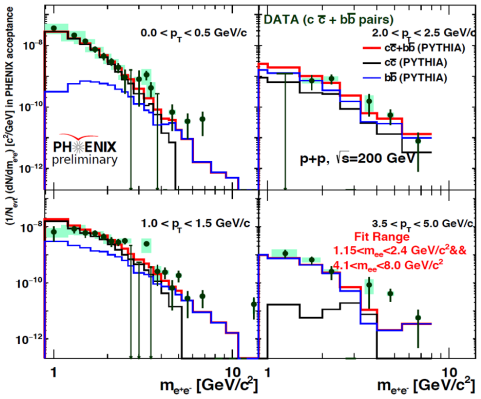


**Figure 8.** Double differential $e^+e^-$ pair yields from heavy flavor decays fitted to simulated distributions from MC@NLO in four $p_T$ bins. Black: $c\bar{c}$ yield, blue: $b\bar{b}$ yield, red: the sum.

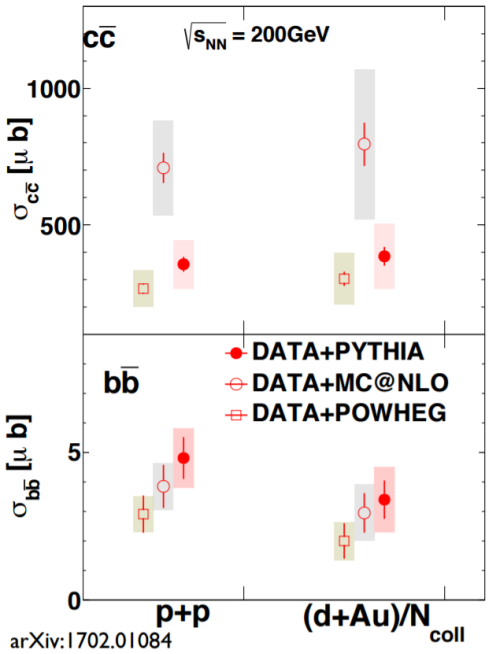


**Figure 9.** The extracted cross-sections of $c\bar{c}$ (top) and $b\bar{b}$ (bottom) in $p + p$ (left) and $d + Au$ (right) collisions. The $d + Au$ cross-section has been scaled down by number of binary collisions $N_{coll}$ to represent the equivalent nucleon-nucleon cross-section. cross-section obtained using PYTHIA, POWHEG, and MC@NLO models.

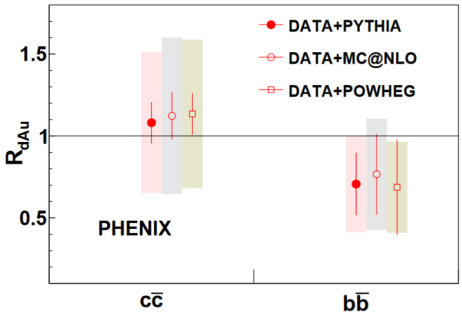


**Figure 10.** The nuclear modification factor $R_{dAu}$ of $c\bar{c}$ and $b\bar{b}$ pairs constructed using cross-sections. The $d + Au$ cross-sections are scled by number of binary collisions $N_{coll} = 7.6 \pm 0.4$.

## References

[1] M. Jacob and G. C. Wick, Ann. Phys. **7**, 404 (1959)
[2] J. C. Collins and D. E Soper, Phys. Rev. **D16**, 2219 (1977)
[3] K. Gottfried and J. D. Jackson, Nuovo Cimento, **33**, 309 (1964)
[4] H. S.Chung, S. Kim, J. Lee, and C. Yu, Phys. Rev. D **83**, 037501 (2011)
[5] H.-S. Shao, H. Han, Y.-Q.'Ma, C. Meng, Y.-J. Zhang, and K.-T. Chao, J. High Energy Phys. **05**, 103, (2015)
[6] A. Adare et al., (PHENIX Collaboration), Phys. Rev. Lett. **1**07, 142301 (2013)
[7] A. Adare et al., (PHENIX Collaboration), Phys. Rev. Lett. **1**11, 202301 (2013)
[8] B. Abelev et al., (ALICE Collaboration), J. High Energy Phys. **1**412, 73 (2014)
[9] A. Adare et al., (PHENIX Collaboration) Phys. Rev. C **9**1, 014907 (2015)
[10] T. Sjostrand, S. Mrenna, and P. Z. Skands, J. High Energy Phys. **5**, 026 (2006)
[11] S. Frixione, P. Nason, and G. Ridolfi, J. High Energy Phys. **0**9, 0126 (2007)
[12] S. Frixione and B. Webber, J. High Energy Phys. **6**, 029 (2002)